

# Effect of charge delocalization on radical ion pair electronic coupling

Louise E. Sinks, Emily A. Weiss, Jovan M. Giaimo, Michael R. Wasielewski \*

*Department of Chemistry, Center for Nanofabrication and Molecular Self-Assembly, Northwestern University,  
2145 North Sheridan Road, Evanston, IL 60208-3113, USA*

Received 24 November 2004; in final form 8 January 2005

## Abstract

Photoinduced charge separation and recombination were studied in a series of covalent donor–acceptor triads consisting of aniline, 1-aminonaphthalene, or 9-aminoanthracene donors (D) attached to a 4-aminonaphthalene-1,8-dicarboximide chromophore (ANI), which in turn is attached to a naphthalene-1,4:5,8-bis(dicarboximide) acceptor (NI) to give D–ANI–NI. The relationship between the molecular structure of  $D^{+\bullet}$  and the magnitude of the electronic coupling between the radicals within  $D^{+\bullet}$ –ANI–NI $^{-\bullet}$  was probed by direct measurements of the spin–spin exchange interaction,  $2J$ , using magnetic field effects on the yield of the neutral triplet state resulting from charge recombination and by density functional theory calculations.

© 2005 Elsevier B.V. All rights reserved.

## 1. Introduction

One of the fundamental issues in developing an understanding of intramolecular electron transfer reactions is the influence of the electronic structures of the redox centers on this process. This structure–function relationship is inadequately captured by many theoretical treatments of electron transfer, which tend to describe a donor or acceptor by only a few quantities such as redox potentials and excited state energies [1]. Two molecules with similar redox and excited state properties may not be equally good electron donors due to other considerations such as competitive relaxation pathways or differences in electron density at the site connecting the donor to the acceptor [2]. While the electronic structure difference is formally incorporated into electron transfer theory via the quantity  $V_{DA}$ , the donor–acceptor electronic coupling matrix element [3,4], this quantity is difficult to predict *ab initio*. However, a qualitative understanding of the relationship between electronic structure and elec-

tronic coupling can be exceptionally useful in designing efficient charge separation systems.

It has been shown that the structural dynamics of the 4-aminonaphthalene-1,8-dicarboximide (ANI) chromophore and the nature of the charge transfer state created by its photoexcitation have a dramatic effect on the electron transfer process [5,6]. The analogous aminonaphthalenes are well known to possess intramolecular charge transfer (ICT) states [7–9]. Upon photoexcitation they quickly form a charge transfer state in which significant positive charge is localized on the amino group and negative charge is located in the naphthalene. Many researchers believe this state is a classic twisted intramolecular charge transfer (TICT) state, where rotation of the amino group localizes positive charge on the nitrogen atom [8], while other groups believe that the trapping mechanism is planarization of the nitrogen (PICT) and not twisting of the amine [7]. Photoexcitation of the ANI chromophore also yields a charge transfer state in which the naphthalene-1,8-bis(dicarboximide) is much more electron deficient than naphthalene. By polarizing the charge density within the ANI chromophore following photoexcitation, electron transfer to an acceptor attached to the naphthalene-1,8-

\* Corresponding author. Fax: +1 847 467 1425.

E-mail address: [wasielew@chem.northwestern.edu](mailto:wasielew@chem.northwestern.edu) (M.R. Wasielewski).

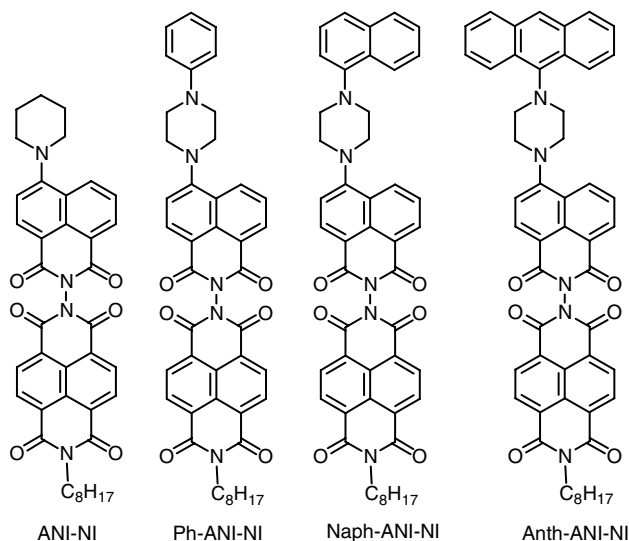


Chart 1. Structures of ANI–NI and D–ANI–NI molecules.

bis(dicarboximide) and hole transfer to a donor attached to the amino group become more favorable.

A series of covalent molecular triads having an aromatic amine electron donor (D), an ANI chromophore, and a naphthalene-1,4:5,8-bis(dicarboximide) acceptor (NI) was synthesized, Chart 1. The donor D is linked to ANI using a piperazine molecule, which furnishes the nitrogen atom of the ANI chromophore as well as an amino group to which aromatic donors, which vary in size from phenyl (Ph) to naphthalene (Naph) and anthracene (Anth), are attached. We wish to explore how increasing the size of the aromatic  $\pi$  system of the secondary donor influences the electron transfer dynamics of the triad systems, D–ANI–NI in toluene. Charge separation and recombination rates are measured using femtosecond and nanosecond transient absorption spectroscopy, respectively. In addition, the magnitude of the electronic coupling between the oxidized donor and the reduced acceptor is probed specifically by direct measurements of the radical ion pair (RP) spin–spin exchange interaction (singlet–triplet splitting),  $2J$ , using magnetic field effects (MFEs) on the yield of triplet states resulting from radical ion pair recombination. The MFEs are due to the Radical Pair InterSystem Crossing (RP-ISC) mechanism, which is well-known to account for triplet production within photosynthetic reaction centers [10–15], and has been described in detail elsewhere [16–25]. The ground and excited state geometries of these molecules were studied using density functional theory.

## 2. Experimental

### 2.1. Computational methods

The donor structures were energy minimized as both neutral and radical cation species with density func-

tional theory (DFT) calculations within the Jaguar electronic structure software package (Jaguar, v. 5.0, Schrödinger, Inc.) using the B3LYP hybrid functional [26,27] and a 6-31G\* basis set. The radical cation spin densities were also calculated with DFT (B3LYP, 6-31G\*) for optimized structures. The optimized geometries of the NI radical anion and the uncharged donor–acceptor molecules were calculated via the PM3 method implemented in Hyperchem (Hypercube, Inc., Gainesville, FL).

The distance between donor–cation and acceptor–anion,  $r_{DA}$ , was calculated by dividing the molecule into two parts, the anion (NI) and the cation (D–ANI). For the anion, the spin density-weighted average of distances to the terminal imide that joins the anion to the cation was calculated to be 3.35 Å. For the cation, the spin density-weighted average of distances to the naphthalene-1,8-dicarboximide part of ANI were calculated. This distance varied with the donor. The reported  $r_{DA}$  is the sum of these two calculations plus the length of the imide–imide bond found for the neutral molecules (1.46 Å).

The internal reorganization energy was calculated using PM3 single point calculations on the DFT-optimized structures for the donor and the acceptor in the uncharged and charged states [21]. The donor molecule utilized the D–ANI geometries; however, the ANI portion was truncated.

This piece-wise calculation of the anion and cation allow for the computational work on the variable part of the molecule (the donor) to be performed at a higher level of theory than the other parts.

### 2.2. Experimental methods

The syntheses of ANI–NI, Ph–ANI–NI, Naph–ANI–NI, and Anth–ANI–NI follow procedures described earlier [19]. *N*-(1-naphthyl)piperidine and *N*-(9-anthryl)piperidine were prepared using Pd(0) catalyzed cross coupling of piperidine to the corresponding bromoaromatics [28]. The magnetic field effect measurements were performed using a previously reported procedure [19–21]. The femtosecond transient absorption apparatus and measurement techniques have also been reported elsewhere [29].

## 3. Results and discussion

### 3.1. Electrochemistry

The photophysics of rod-like donor–acceptor arrays containing the ANI chromophore have been characterized previously in detail [6]. The redox properties of this series of molecules are presented in Table 1. All potentials are reported vs. SCE. All measurements were performed in dichlorometh-

Table 1  
Oxidation ( $E_{\text{ox}}$ ) and reduction ( $E_{\text{red}}$ ) potentials vs. the saturated calomel electrode

Compound	$E_{\text{ox}}$	$E_{\text{red}}$
NI		-0.63
ANI	1.2	
Ph-ANI	1.07	-1.32
Naph-ANI	1.09	-1.35
Anth-ANI	0.93	-1.36

ane (DCM) with 0.1 M tetra-*n*-butylammonium hexafluorophosphate (TBAPF<sub>6</sub>) as a supporting electrolyte, with a ferrocene internal standard (0.475 V vs. SCE). The acceptor, NI, reduces at -0.63 V, and the ANI donor oxidizes at 1.2 V. Ph-ANI and Naph-ANI have similar oxidation potentials, 1.07 and 1.09 V, respectively, while the Anth-ANI is somewhat easier to oxidize, 0.93 V. The oxidation potentials of the D-ANI compounds are less positive than that of ANI due to resonance stabilization of the aromatic amine radical cations.

### 3.2. Geometries and spin densities

Comparison of the DFT geometries of D-ANI and D<sup>+</sup>-ANI<sup>-</sup> indicates that the structural features that change most across the series are the dihedral angles between the aromatic ring of D and the piperazine, see Fig. 1. These two dihedral angles, D1 and D2, as well as the dihedral angles describing the piperazine-ANI attachment, D3 and D4, are listed in Tables 2 and 3.

The ground state geometries show that the dihedral angle between the donor group and the piperazine ring increases as the aromatic D group gets larger. This presumably minimizes steric interactions. In the case of the smallest donor where

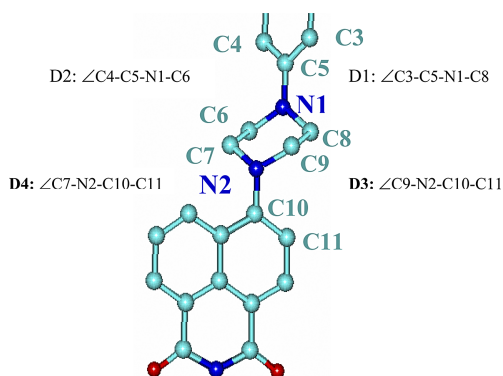


Fig. 1. A schematic representation of the dihedral angles of the system.

Table 2  
Dihedral angles of the neutral compound, see Fig. 1

Compound	D1	D2	D3	D4
Ph-ANI-NI	11.1	55.7	23.9	59.9
Naph-ANI-NI	77.0	29.0	25.6	60.9
Anth-ANI-NI	72.0	108	24.4	59.5

Table 3  
Dihedral angles of the radical cation, see Fig. 1

Compound	D1	D2	D3	D4
Ph-ANI-NI	11.0	35.3	26.3	54.6
Naph-ANI-NI	34.1	45.4	26.9	57.2
Anth-ANI-NI	52.9	47.8	27.8	62.1

D = Ph, there is relatively little steric interaction and the D group is fairly planar with respect to the piperazine ring (D1 = 11.0°, D2 = 55.7°). The bulky anthracene group resides in a nearly perpendicular orientation (D1 = 72.0°, D2 = 108.4°), while the naphthalene case is intermediate (D1 = 77.0°, D2 = 29.0°). The dihedral angles describing the amino to naphthalene-1,8-dicarboximide link are fairly constant throughout the series with D3 ~ 24° and D4 ~ 60°.

The minimized radical cation structure depends not only on steric hindrance, but also on changes in electronic structure. These factors are competing; steric factors dictate that the D-piperazine connection be close to perpendicular while electronic considerations strongly favor planarization of the system to distribute charge over the largest possible conjugated  $\pi$  system. We see that the electronic interaction is dominant; all compounds are significantly more planar in their radical cation state than their ground state. However, within the series, steric bulk does have an impact on how planar the system can become. The trend is similar to that seen in the ground state: the phenyl donor is more planar than the bulky anthracene donor. Again, the D3 and D4 dihedral angles change little across the series.

The spin densities for the radical cations are summarized in Table 4, which lists the percent spin density at each nitrogen atom in the piperazine, the percent spin density summed over each carbon in Ph, Naph, or Anth, and the total percent spin density in those three regions. In all cases, the majority of the spin density is located in those three places (Total); however, the amount delocalized throughout the rest of the system does change. When D = Ph, 65% of the spin density is located on the aniline or piperazine nitrogens and 35% is located elsewhere in the system. When D = Naph, 30% is located elsewhere in the system, and for D = Anth only 19% is localized elsewhere. As the cation structure becomes less planar, the charge becomes more localized on the D = aromatic and piperazine nitrogens. As we increase the size of the  $\pi$  system, the charge is stabilized better by delocalizing exclusively through the  $\pi$  system without needing additional conjugation with the naphthalene-1,8-dicarboximide portion of the system. This is clearly seen in the spin densities: Ph-ANI has 19% localized in the phenyl, Naph-ANI has 41% in the naphthalene donor, and Anth-ANI has 60% of the spin density on the anthracene

Table 4  
Quantities calculated from the spin densities of the radical cations on geometry optimized structures, see Fig. 1

Compound	Spin density (%)				$r_{\text{DA}}$
	N1	N2	Aromatic system	Total	
Ph-ANI-NI	31	15	19	65	12.4
Naph-ANI-NI	18	11	41	70	13.4
Anth-ANI-NI	15	6	60	81	15.1

moiety. Additionally, the density on the piperazine nitrogens shifts toward the aromatic donor as the size of the  $\pi$  system increases.

It is clear that the bulk of the spin density does move toward the D moiety as the size of the aromatic system increases, and this is captured by the  $r_{DA}$  we computed as described in the experimental and listed in Table 4. This will be an important metric for understanding the magnetic field effect results.

### 3.3. Photophysics

Femtosecond transient absorption spectroscopy indicates that charge separation occurs via a two-step mechanism for all compounds. In all cases, fast electron transfer occurs between ANI and NI to form  $D-ANI^+-NI^-$  with  $\tau = 1.0-1.2$  ps. This is followed by a fast charge shift from  $ANI^+$  to the secondary donor, D with  $\tau = 3-8$  ps. The final ion pair,  $D^+-ANI-NI^-$ , lives longer than the initial ion pair,  $D-ANI^+-NI^-$  in all cases, Table 5. Representative transient absorption spectra for Anth-ANI-NI are shown in Fig. 2. At the earliest time,  $t = 0.36$  ps, the ground state bleach of ANI is apparent at 400 nm along with the 490 nm feature which is indicative of  $^1AN^*$  [6]. These two features rapidly disappear, and by  $t = 1.04$  ps the spectrum shows the prominent  $NI^-$  bands at 480 and 610 nm. Charge recombination times generally increase as  $r_{DA}$  increases. However, charge recombination within  $Naph^+-ANI-NI^-$  is somewhat slower than within  $Anthr^+-ANI-NI^-$  due to energetic considerations. The time constants for charge separation, charge shift and charge recombination are reported in Table 5.

Table 5  
Summary of photophysics in toluene

Compound	$\tau_{CS}$ (ps)	$\tau_{CR}$ (ns)	$2J$ (mT)
ANI-NI	0.7	12.0	–
Ph-ANI-NI	1.2, 3	17.0	–
Naph-ANI-NI	1.3, 5	37.1	26
Anth-ANI-NI	1.0, 8	30.4	17

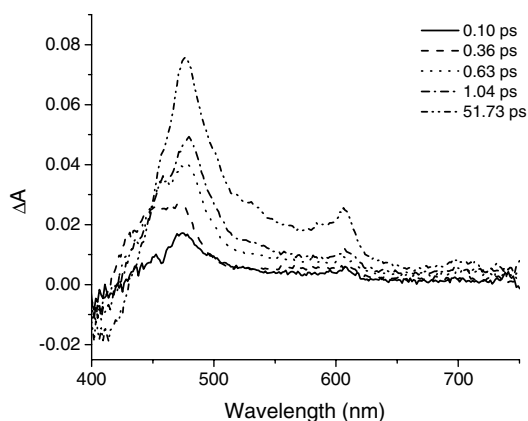


Fig. 2. Transient spectra of Anth-ANI-NI in toluene following a 400 nm, 100 fs laser flash.

### 3.4. The magnetic field effect

Extensive descriptions of the influence of magnetic fields on radical pair spin dynamics of organic systems have been published recently by Weiss et al. [19–21]. Briefly, when the electron transfer reaction originates from a state in which the redox centers are also paramagnetic, e.g., charge recombination from a radical pair (RP), the electronic coupling that dictates charge transfer from the RP to energetically proximate electronic states is also that which facilitates the magnetic interaction between the unpaired spins of the RP [30–34]. Therefore, the magnitude of the magnetic interaction and its behavior as a function of donor–acceptor distance should precisely mirror that of  $V_{DA}^2$ .

Immediately following rapid, nonadiabatic charge separation, the correlated electron spins are in a singlet configuration. Following their formation, the weakly coupled electron spins are free to precess independently around the resultant of their respective local fields due mainly to the electron–nuclear hyperfine interactions and the external applied magnetic field. After times usually in the range of a few nanoseconds, RP-ISC results in the formation of a triplet spin configuration. When hyperfine and exchange interactions are isotropic and spin–spin coupling is weak, each of the three zero-field triplet states of the radical pair will be nearly degenerate with the singlet and will be populated with equal probability at room temperature. If the spin–spin exchange interaction within the radical ion pair is nonzero, the triplet manifold is not initially degenerate with the singlet, but rather separated from the singlet by an energy  $2J$ , Fig. 3.

Application of a magnetic field results in Zeeman splitting of the triplet sublevels, which at high fields can be described by the  $T_0$  and  $T_{\pm 1}$  states, Fig. 3. In the high field limit, population of the RP triplet state occurs exclusively by  $S-T_0$  mixing, while  $T_{-1}$  and  $T_{+1}$  remain unpopulated. Electron paramagnetic resonance (EPR) measurements on closely related compounds have confirmed that the triplet levels of the radical pair are higher in energy than the singlet state as would be expected from net antiferromagnetic exchange [35]. When the Zeeman energy from the applied field equals that of the  $S-T$  splitting, the low energy triplet state,  $T_{-1}$ , crosses the singlet, and the RP-ISC rate is maximized, which

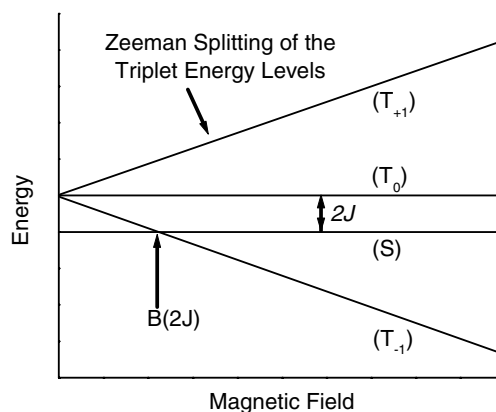


Fig. 3. Schematic of radical ion pair energy levels as a function of magnetic field.

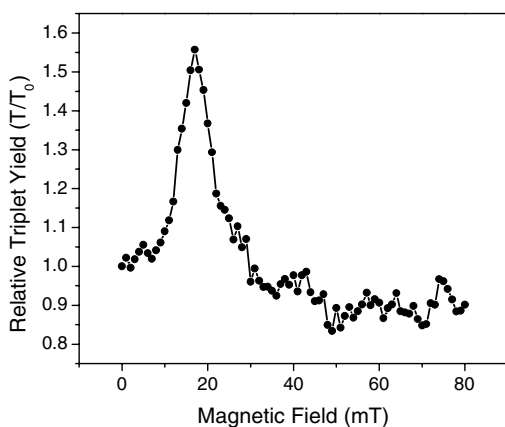


Fig. 4. Relative yield of  $^3\text{*NI}$  vs. magnetic field for Anth-ANI-NI in toluene.

produces a resonance in the triplet yield at  $B_{2J}$ . The results of the magnetic field effect experiments are summarized in Table 5. ANI-NI and Ph-ANI-NI both have values of  $2J$  that are larger than we can measure ( $>1$  T). Naph-ANI-NI has a  $2J$  value of 26 mT, while Anth-ANI-NI has  $2J = 17$  mT, Fig. 4. It should be noted that, although Ph-ANI-NI has a very similar  $r_{\text{DA}}$  to that of the meta-linked 6ANI-Ph-NI molecule in [25], the  $2J$  value for Ph-ANI-NI is at least a factor of 3 ( $>1$  T) greater than that of 6ANI-Ph-NI ( $2J = 320$  mT). This is most likely due to the fact that in 6ANI-Ph-NI, there are two near-orthogonal phenyl-imide linkages between donor and acceptor, and in Ph-ANI-NI, there is a single orthogonal imide-imide linkage between 6ANI and NI. Large dihedral angles between chromophores reduce electronic coupling significantly by breaking the conjugation between donor and acceptor. The observed decrease in  $2J$  correlates well with the value of  $r_{\text{DA}}$  determined from our electronic structure calculations. Although, we only have two  $2J$  values, we may calculate a decay parameter, ( $2J = 2J_0 \exp(-\alpha r_{\text{DA}})$ ),  $\alpha = 0.25 \text{ \AA}^{-1}$  for these two points. Because  $2J \propto V_{\text{DA}}^2$ , the parameter for the exponential decay of the coupling,  $\beta = \alpha/2 = 0.13 \text{ \AA}^{-1}$ . This weak dependence of coupling on distance is very reasonable considering that the extension of the conjugated  $\pi$ -system, rather than the addition of any weakly-coupling  $\sigma$ -bond linkages, is responsible for the increase in  $r_{\text{DA}}$ .

#### 4. Conclusion

We are able to exploit the intramolecular charge transfer character of our primary donor, ANI, to create longer-lived radical ion pair states. By modifying the nature of the 4-amino group on ANI, we are able to localize the positive charge at greater distances from the radical anion, thus prolonging the lifetime of the ion pair state. As the distance between the radical cation and the radical anion increases, the cation becomes trapped on the donor, and their electronic coupling to one another decreases. The electronic stabilization of the radical cation in the  $\pi$  systems of the larger donors

occurs despite the less than favorable radical cation geometry due to steric constraints.

#### Acknowledgments

This work was supported by the Division of Chemical Sciences, Office of Basic Energy Sciences, U.S. Department of Energy under Grant No. DE-FG02-99ER-14999. E.A.W. thanks the Link Foundation for support. The authors thank Dr. Michael J. Tauber for many helpful discussions.

#### References

- [1] A. Weller, *Z. Phys. Chem. (Munich)* 133 (1982) 93.
- [2] R.T. Hayes, C.J. Walsh, M.R. Wasielewski, *J. Phys. Chem. A* 108 (2004) 3253.
- [3] R.A. Marcus, *J. Chem. Phys.* 24 (1956) 966.
- [4] R.A. Marcus, N. Sutin, *Biochim. Biophys. Acta* 811 (1985) 265.
- [5] L.E. Sinks, M.R. Wasielewski, *J. Phys. Chem. A* 105 (2003) 611.
- [6] S.R. Greenfield, W.B. Svec, D. Gosztola, M.R. Wasielewski, *J. Am. Chem. Soc.* 118 (1996) 6767.
- [7] S. Saha, A. Samanta, *J. Phys. Chem. A* 106 (2002) 4763.
- [8] K. Suzuki, H. Tanabe, S. Tobita, H. Shizuka, *J. Phys. Chem. A* 101 (1997) 4496.
- [9] F. Lahmani, E. Breheret, O. Benoist d'Azy, A. Zehnacker-Rentien, J.F. Delouis, *J. Photochem. Photobiol. A* 89 (1995) 191.
- [10] R. Haberkorn, M.E. Michel-Beyerle, *Biophys. J.* 26 (1979) 489.
- [11] R. Haberkorn, M.E. Michel-Beyerle, R. Marcus, *Proc. Natl. Acad. Sci. USA* 76 (1979) 4185.
- [12] A.J. Hoff, H. Rademaker, R. Van Grondelle, L.N.M. Duysens, *Biochim. Biophys. Acta* 460 (1977) 547.
- [13] A.J. Hoff, *Photochem. Photobiol.* 43 (1986) 727.
- [14] M.E. Michel-Beyerle, H. Scheer, H. Seidlitz, D. Tempus, *FEBS Lett.* 110 (1979) 129.
- [15] P.J. Hore, D.A. Hunter, C.D. McKie, *Chem. Phys. Lett.* 137 (1987) 495.
- [16] R.E. Blankenship, T.J. Schaafsma, W.W. Parson, *Biochim. Biophys. Acta* 461 (1977) 297.
- [17] K. Schulten, H. Staerk, A. Weller, H. Werner, B. Nickel, *Z. Phys. Chem. (Munich)* 101 (1976) 371.
- [18] U. Till, P.J. Hore, *Mol. Phys.* 90 (1997) 289.
- [19] E.A. Weiss, M.A. Ratner, M.R. Wasielewski, *J. Phys. Chem. A* 107 (2003) 3639.
- [20] E.A. Weiss, M.J. Ahrens, L.E. Sinks, A.V. Gusev, M.A. Ratner, M.R. Wasielewski, *J. Am. Chem. Soc.* 126 (2004) 5577.
- [21] E.A. Weiss, L.E. Sinks, A.S. Lukas, E.T. Chernick, M.A. Ratner, M.R. Wasielewski, *J. Phys. Chem. B* 108 (2004) 10309.
- [22] Y. Mori, Y. Sakaguchi, H. Hayashi, *J. Phys. Chem. A* 104 (2000) 4896.
- [23] A. Weller, H. Staerk, R. Treichel, *Faraday Discuss. Chem. Soc.* 78 (1984) 271.
- [24] A. Weller, F. Nolting, H. Staerk, *Chem. Phys. Lett.* 96 (1983) 24.
- [25] A.S. Lukas, P.J. Bushard, E.A. Weiss, M.R. Wasielewski, *J. Am. Chem. Soc.* 125 (2003) 3921.
- [26] C. Lee, W. Yang, R.G. Parr, *Phys. Rev. B* 37 (1988) 785.
- [27] A.D. Becke, *J. Chem. Phys.* 98 (1993) 5648.
- [28] M. Nishiyama, T. Yamamoto, Y. Koie, *Tetrahedron Lett.* 39 (1998) 617.

- [29] B. Rybtchinski, L.E. Sinks, M.R. Wasielewski, *J. Phys. Chem. A* 108 (2004) 7497.
- [30] P.W. Anderson, *Phys. Rev.* 79 (1950) 350.
- [31] P.W. Anderson, *Phys. Rev.* 115 (1959) 2.
- [32] H.A. Kramers, *Physica* 1 (1934) 182.
- [33] J.S. Miller, A.J. Epstein, W.M. Reiff, *Acc. Chem. Res.* 21 (1988) 114.
- [34] J. Yamashita, J. Kondo, *Phys. Rev.* 109 (1958) 730.
- [35] K. Hasharoni, H. Levanon, S.R. Greenfield, D.J. Gosztola, W.A. Svec, M.R. Wasielewski, *J. Am. Chem. Soc.* 117 (1995) 8055.